Applied Physics A (2023) 129:401
https://doi.org/10.1007/s00339-023-06620-2

Applied Physics A
Materials Science & Processing

Neisseria meningitidis detection by coupling bacterial factor H onto Au/scFv antibody nanohybrids

Maryam Rad[1] · Gholamhossein Ebrahimipour[1] · Mojgan Bandehpour[2,3,4] · Omid Akhavan[5] · Fatemeh Yarian[2,3,6]

Received: 13 September 2022 / Accepted: 2 April 2023 / Published online: 8 May 2023

Abstract

Neisseria meningitides is one of the causative agents of the deadly bacterial meningitis disease, and its rapid diagnosis is highly required. In this study, at first, a specific single-chain variable fragment (scFv) antibody-conjugated Au NPs with average size of ~ 20 nm and surface plasmon resonance absorption peak at ~ 530 nm in wavelength were synthesized. Then, the NPs were loaded on nitrocellulose membrane pads for designing a selective lateral flow immunoassay test strip which is sensitive to the factor H protein of *Neisseria meningitidis*. The results showed a minimum detectable bacterial concentration of 0.5 µg/mL in only three minutes. The molecular structure of the scFv antibody-Au NPs (with the binding energy of − 4.7 kcal) has been also investigated by docking method. Furthermore, the complex *Z*-score (− 7.47) calculated by using ProSA software confirmed that our protein is in the range of all known Z-scores of the protein structures.

Graphical abstract

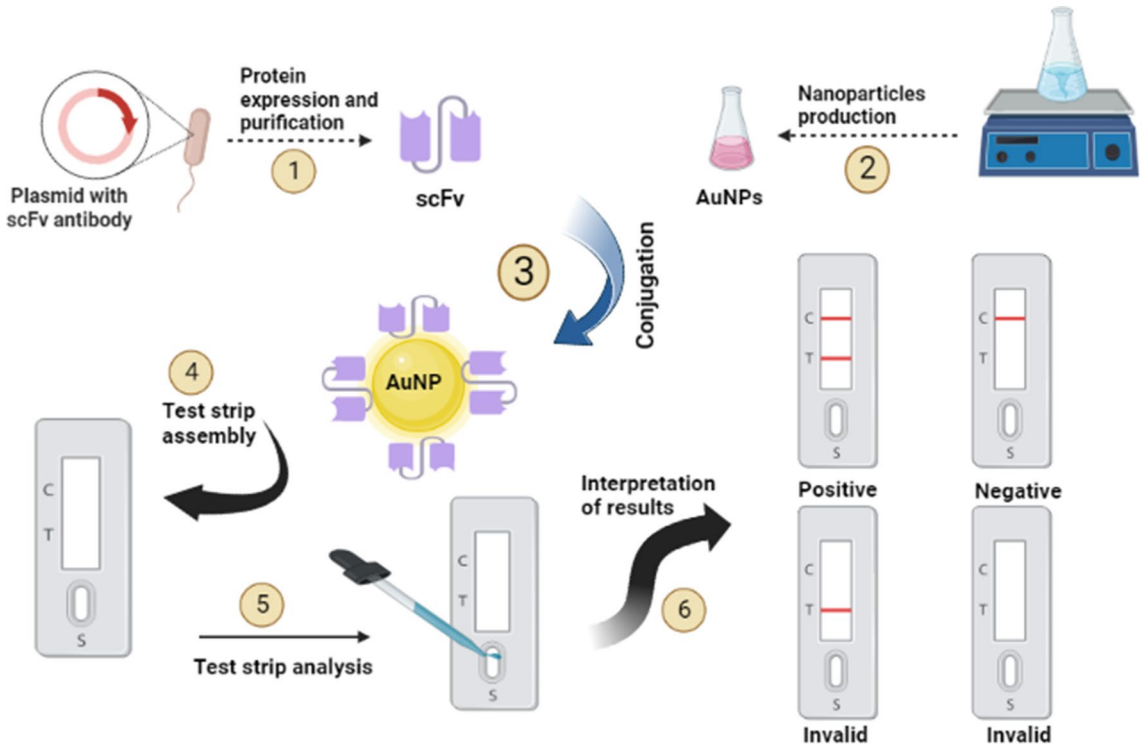

Keywords Nanomaterials · Gold nanoparticles · Bacterial sensors · Plasmon resonance · Recombinant antibody · Test strips

Extended author information available on the last page of the article

1 Introduction

Two and a half million people worldwide are infected with meningitis, so that it killed nearly 319,000 people in 2016 [1]. Meningitis is one of the leading causes of death in developing countries, with a 4–27% mortality rate. Although the prevalence of the disease is sporadic in most cases, it causes anxiety in local communities [2]. Many pathogens, such as bacteria, viruses, fungi, and parasites, cause meningitis [1]. In fact, four bacteria of *Haemophilus influenzae* type b (Hib), *Streptococcus pneumoniae, Neisseria meningitidis, and Streptococcus agalactiae* are responsible for 90% of bacterial meningitis in the world [3]. Meningococcal meningitis can be a life-threatening disease in different age groups causing permanent damage to the central nervous system and death within a few hours due to the sudden onset of symptoms and rapid progression of the disease [4]. Hence, the development of rapid diagnostic systems becomes more important in critical situations where disease monitoring and management are critical.

Nanoparticles are of interest in various fields [5, 6] and are used to improve the specificity and sensitivity of diagnostic methods of biomolecules [7]. Among the various nanoparticles, gold nanoparticles (Au NPs) are very important in clinical diagnosis, due to their physicochemical properties, powerful colors, high absorption, and cross-sectional scattering properties that come from the its unique surface plasmon resonance (SPR) characteristic. The SPR properties of Au NPs have been resulted in their wide applications form optical properties [8] to biomedical applications [9].

The development of several colorimetric detection methods based on Au NPs stems from these characteristics. Biocompatibility, optical and electronic properties, and relatively simple production, and modification are the special characteristics that have led to the applications of Au NPs in the field of biosensors [10].

Polyclonal, monoclonal, and recombinant antibodies are used for designing Au NP-based biosensors [11]. Antibodies can bind to Au NPs by covalent, electrostatic, and/or hydrophobic bonding. For a simple as well as general application, the optical properties of Au NPs and antibodies can be combined into a probe on a test strip using the immunoassay method to design a rapid test [12]. Hence, the goal of this study is rapid, simple and selective diagnosis of *Neisseria meningitidis* by a user-friendly test strip. In this regard, a home-made single chain variable fragment (scFv) antibody [13] was firstly prepared. Then, the scFv recombinant antibody-conjugated Au NPs were synthesized and loaded on a nitrocellulose membrane pad for designing a lateral flow assembly test strip detecting the bonding of *Neisseria meningitidis* bacterial (fHbp) antigen to the scFv/Au NPs. The molecular structure of the scFv recombinant antibody-Au NPs has been also investigated by using docking method and the Z-score calculation.

2 Experimental

All experimental protocols were approved by the Shahid Beheshti University of Medical Sciences Ethics Committee [Code of Ethics: IR. SBMU.RETECH.REC.1400.080]. Biochemical materials containing isopropyl β-D-1-thiogalactopyranoside (IPTG) ($C_9H_{18}O_5S$), trisodium citrate ($Na_3C_6H_5O_7$), acrylamide (C_3H_5NO), imidazole ($C_3H_4N_2$), Tris ($NH_2C(CH_2OH)_3$), urea ($CO(NH_2)_2$), and chloroauric acid ($HAuCl_4$) were procured from the Sigma Aldrich (3050 Spruce St. Louis, MO, USA) company. Some of the illustrations were prepared by using BioRender.

2.1 Preparation of the fHbp and scFv

Escherichia coli BL21 (DE3) containing recombinant plasmids (pET28a containing the scFv sequence) were prepared in Luria–Bertani medium containing 70 µg/mL kanamycin at a 37 °C culture with an optical density (OD_{600}) of 0.6. First, protein expression was performed by adding 0.5 mM IPTG. SDS-PAGE using 12% polyacrylamide gel was used to evaluate the svFv proteins expression. The samples were then prepared with protein loading (125 mM Tris, 20% glycerol, 4% SDS, 200 mM DTT, and 0.01% bromophenol blue at pH = 6.8) followed by heating at 85 °C for 5 min. A Coomassie brilliant blue R-250 was used to stain the gel. Then, the expressed protein was separated from the 12% polyacrylamide gel for analysis by Western blotting and electrophoretically transferred to a nitrocellulose membrane (Whatman, UK). The membrane was subsequently incubated with a 1: 2000-diluted alkaline phosphatase (ALP)-labeled anti-His tag monoclonal antibody (Abcam, UK) and observed in an NBT/BCIP substrate solution (Roche, Germany). After the pellet was resuspended in 5 mL of denaturing buffer (6 M Urea, 20 mM NaH_2PO_4, and 500 mM NaCl, pH = 8.0) and lysed by sonication on ice, the lysate was transferred to a chromatography Ni^{2+}-NTA agarose resin (Novagen, USA) column for purification of recombinant His-tagged scFvs. The bound antibodies were dialyzed with PBS after separation with an elution buffer (500 mM imidazole, 20 mM NaH_2PO_4, and 500 mM NaCl, pH = 8.0). Finally, the protein was analyzed by Western blotting. Figure 1 schematically shows these steps.

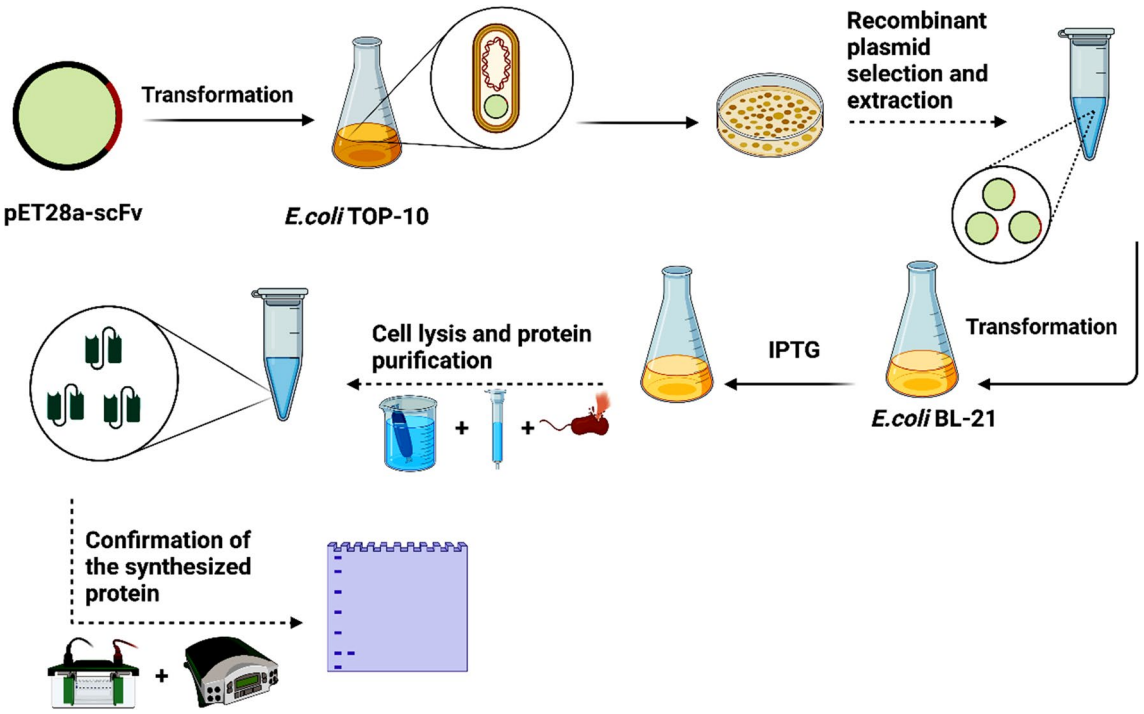

Fig. 1 The schematic representation of the scFv expression and purification. After selecting the recombinant plasmid result from the transformation of pET28a-scFv to *E. coli* TOP10, this plasmid transforms to *E. coli* Bl-21 to express the scFv by adding IPTG. Then, the bacterial cells are lysed and purified by chromatography and dialysis. The result was confirmed with SDS-PAGE and western blot

2.2 Synthesis of gold NPs

Under the Turkevich method [14–18], 25 mL of distilled water was mixed with 250 µL of $HAuCl_4$ (0.1 M) to reach a final concentration of 1 mM hydrochloric acid. The Erlenmeyer flask containing the above solution was placed on a heater stirrer until boiling. Then, the solution was immediately mixed with 2.5 mL of trisodium citrate 38.8 mM, while simultaneously being stirred by a magnet stirrer. After that a red wine color appeared, the solution was left to cool to the room temperature.

2.3 Gold NPs characterizations

An X-ray diffractometer (XRD) in the scanning range of 20°–80° (2θ) equipped by a Cu Ka radiation source operating at wavelength of 1.5406 mA was used to determine the crystallographic structure of the nanoparticles (StoE, Hilpertstrasse, Darmstadt, Germany). The size and morphology of the nanoparticles were determined by field-emission scanning electron microscopy (FESEM, (TESCAN, Brno, Czech Republic). The absorption peak of gold NPs was analyzed with a UV–Vis spectrophotometer (Lambda 25, Perkin Elmer, MA, USA) from 200 to 800 nm of the wavelength range.

2.4 Conjugation of gold NPs to antibodies

3 mL of the gold NP suspension (with concentration of 51.6 µg/mL) was centrifuged at 8000 rpm for 20 min. Then, the precipitate was dissolved in 1 mL of diluted 1X PBS buffer (1:14). 100 µL of the antibodies with the concentration of 100 µg/mL were added to 1 mL of gold NPs suspension and kept overnight at 4 °C. The solution was then centrifuged at 8000 rpm for 20 min to remove unbound antibodies and added to a 1 ml diluted 1X PBS buffer. The results of the binding of gold NPs to the antibody were investigated with a UV–Vis spectrophotometer.

2.5 Test strip assembly

The test strips were assembled by loading the desired materials on nitrocellulose membranes. To create, control, and test the lines, the goat anti-mouse IgG (with concentration 2 mg/mL) and scFv (with concentration 2 mg/mL) were first printed on a nitrocellulose membrane by using a dispenser device (BioDot 17,781, U.S). Then, the membrane was placed at 37 °C for 2 h to fix the antibody. The distance between the control and test lines was considered ~ 4 mm. Next, the sample pad was treated by immersion in a solution (0.01 M PBS, pH 7.4, containing 1% BSA) for 30 min and drying at 37 °C. Finally, an appropriate amount of

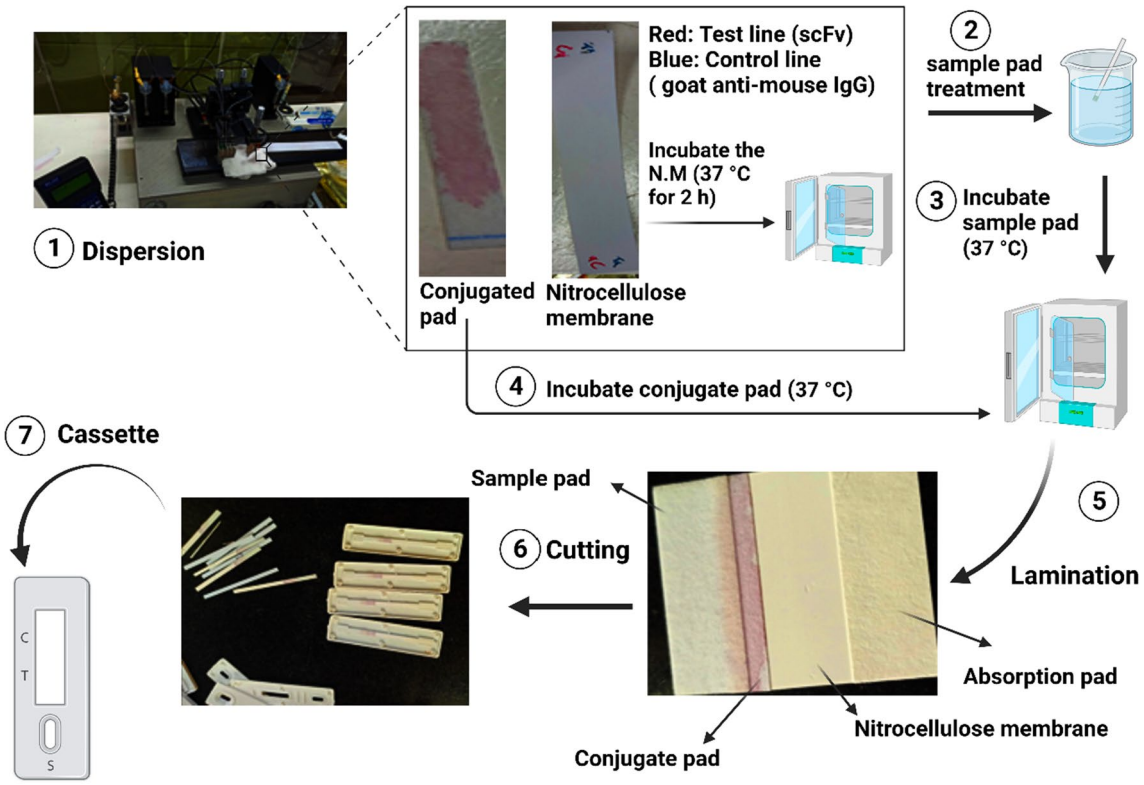

Fig. 2 An illustration of the steps done for the fabrication of the lateral flow assembly

antibody-conjugated Au NPs was printed on the conjugate pad and dried at 37 °C. The prepared set was placed on a backing card. These steps are shown in Fig. 2.

2.6 Test strip analysis

The test strips were exposed to a *Neisseria meningitidis* pseudo lysate medium, as a positive specimen, and *Escherichia coli* lysates (obtained from *E. coli* BL21 (DE3) and *E. coli* TOP10 as a strain of *E.coli* K-12 [19] as a non-pathogen strain model [20]), as a negative control. Two different concentrations (0.5 and 1 µg/mL) of positive and negative samples were used to analyze the diagnostic tests. The results were evaluated based on the red color detected in the control line and/or test line area. The detailed steps are presented in Fig. 3.

2.7 Docking of gold nanoparticles to antibodies

The scFv amino acid sequences was first given to the Iterative Threading Assembly Refinement (I-TASSER) server. The protein with the highest c-score was selected from the obtained data and then loaded on a three-dimensional refine server to modify the protein structure. Next, the energy minimization was carried out by the molecular graphics, modeling, and simulation program (Yasara Model approval was checked on the "saves.mbi.ucla.edu" site. Then, the *Z*-score was determined on the Prosa site. Following that, the protein and ligand structure was screened in Pyrx software, and the interaction energy was evaluated. Finally, the resulting complex was investigated in discovery studio software.

3 Results and discussion

Many rapid diagnostic tests have been designed to detect bacteria [21] and specifically meningitis [22, 23]. Problems such as high cost, the need for a cold cycle, cross-reactivity with other bacteria, and the need for experienced staff are disadvantages of the latex agglutination tests. The need for high sample volumes is also a limitation of immunochromatographic tests. Other disadvantages of molecular rapid diagnostic tests include the need for electrical equipment and high cost. Notwithstanding, the World Health Organization's roadmap (Defeating Meningitis by 2030) demonstrates the importance of designing rapid diagnostic tests to identify meningitis [1]. This study aims to provide some method for reducing the above obstacles.

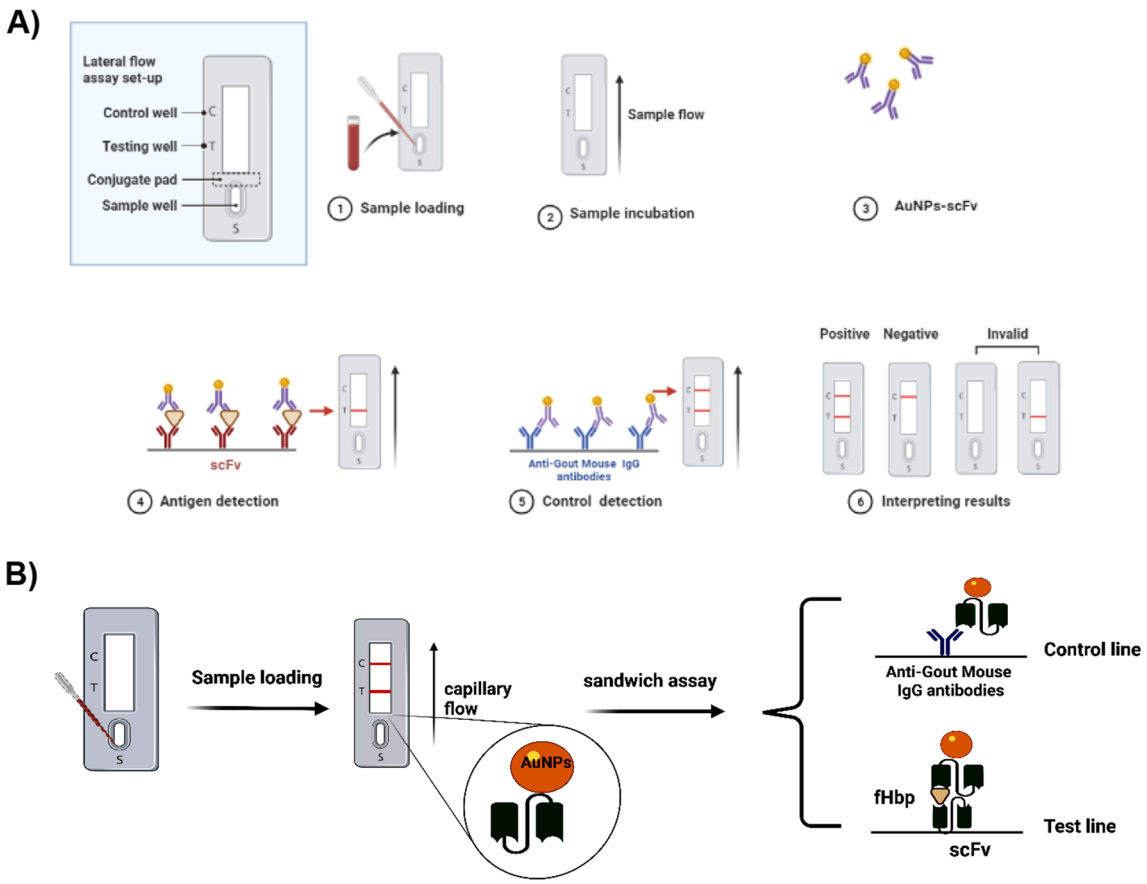

Fig. 3 **A** Illustration of the test strip analysis process and **B** more schematically details of obtaining a positive result. In this process, after reaching out a positive sample solution to the test line, the fHbp binds to the scFv-Au NPs, sandwiches with the scFv fixed in the test line, and then the red colors appeared in the both T and C lines. In the control line, the color appearance was caused by the interaction between the anti-gout mouse IgG antibody and the scFv

3.1 scFv specific antibody characterization

Two important protein identification methods are sodium dodecyl sulfate–polyacrylamide gel electrophoresis (SDS-PAGE) and Western Blot. In the SDS method, the proteins are isolated by size, while in the Western blot method, the proteins are distinguished by their specific antibody [24]. In this regard, Fig. 4 shows the results of SDS-PAGE and Western blotting of the prepared scFv with the weight of 27 KDa, after the expression and purification of the antibody. These results confirmed the sucsseful formation of the scFv recombinant antibody.

3.2 XRD and optical analyses

The crystal structure of gold NPs was studied by XRD analysis. Figure 5a shows diffraction peaks at 2Θ Bragg angles of 38.1, 44.3, 64.5 and 77.7° corresponding to (111), (200), (220) and (311) crystalline planes of an fcc structure for the gold NPs, respectively. The absorption spectrum of the pure

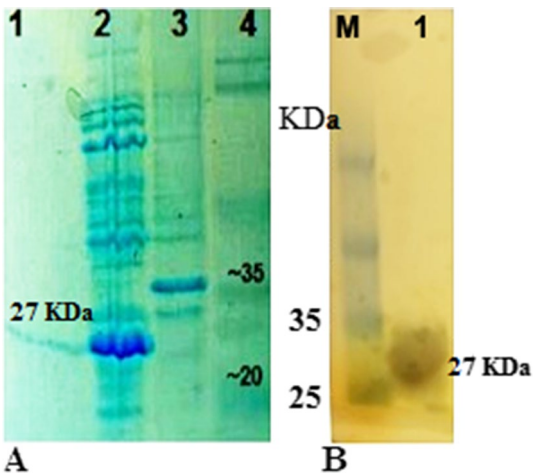

Fig. 4 Recombinant scFv expression. **A** SDS-PAGE analysis of the expressed scFv containing: (1) the purified scFv, (2) the expressed lysate, (3) *E. coli* Bl-21 control lysate, and (4) the protein marker, and **B** the purified scFv Western Blotting with a mss of 27 KDa containing: (M) as the protein marker and (1) as the purified scFv

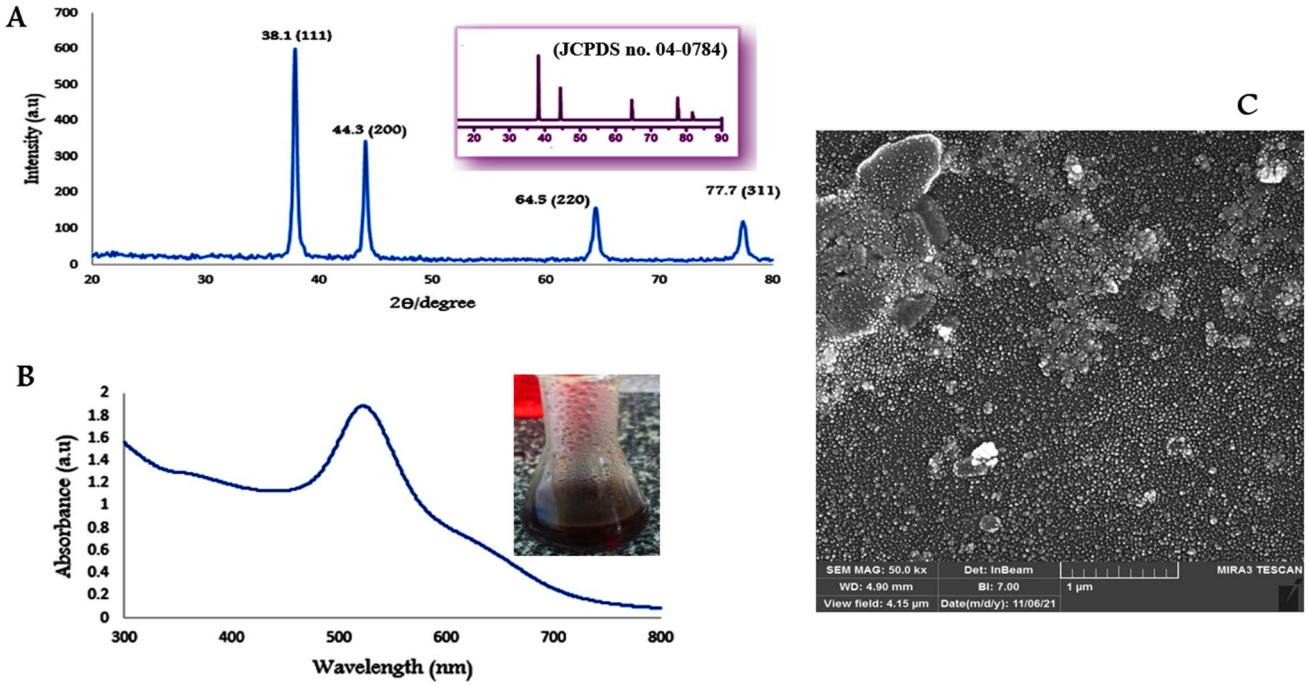

Fig. 5 **A** XRD pattern of the Au NPs. The standard JCPDS card is presented as the inset. **B** UV–Vis spectrum of the Au NPs. The inset shows an optical image of the Au NP suspension presenting a red color, and **C** SEM image of the Au NPs

gold NPs in Fig. 5b shows a SPR peak at 523 nm in wavelength, indicating the formation of gold NPs.

3.2.1 FESEM analysis

Figure 5c shows the FESEM image of the gold NPs. It presents a nearly spherical morphology for the synthesized nanoparticles. The average size of the nanoparticles was found ~ 20 nm, which is a suitable size of gold NPs for designing SPR-based lateral flow assays [25].

3.3 UV–Visible spectroscopy

One way to confirm the binding of gold NPs to antibodies is comparing the absorption peak of naked nanoparticles with that of the conjugated ones. Any red-shift in the location of the SPR peak can be assigned to the conjugation of antibody-nanoparticles [26]. In this work, we found that by adding trisodium citrate to the reaction solution, a red-wine color was obtained, as an evidence confirming formation of gold NPs [27]. Figure 6A shows that conjugation of the NPs to the scFv antibody resulted in a red-shift in the SPR peaks of the NPs from 523 to 532 nm. In fact, the spectroscopic characteristics of the NPs clearly shows a slight increase in the size of the gold NPs due to binding to the antibody causing adaption of the surface plasmon resonance and no significant changes in the spherical shape of the NPs [28]. It should be noted that no aggregation was observed for the functionalized gold NPs during the preparation, storing and applications. This was simply found by observing the stability in the homogeneity as well as the red color of the gold NP suspensions, after the long periods of storing and applications. In fact, the designed test strip not only used the spherical form of gold NPs as the most common forms in lateral flow immunoassay [29], but also the functionalized ones provided a strong signal and high stability, as comared to the unfunctionalized ones [30]. Figure 6B, C show that antigen–antibody binding of the fHbp and scFv on the gold NPs resulted in color change of the suspension from red to brown color, implying formation another conjugation. In fact, red-shift of the PSR peaks due to size increasing and/or accumulating the NPs was previously reported [31].

3.4 Test strip analysis

For the designed test strip, a valid as well as negative result is corresponding to a red color appearanece in the control line. Furthermore, the positive result of the test strip is determined by appearance of the red color of the gold NPs in both the test and control lines. Any absence of the red color indicates the invalidity of the test [32]. In this regard, we have found that three minutes after adding one drop of *Neisseria meningitidis* pseudo lysate to the strip test, the red color was observed in the both test line and control line (see Fig. 7). However, for *Escherichia coli* lysate, only the control line showed the red color (as a negative result). The

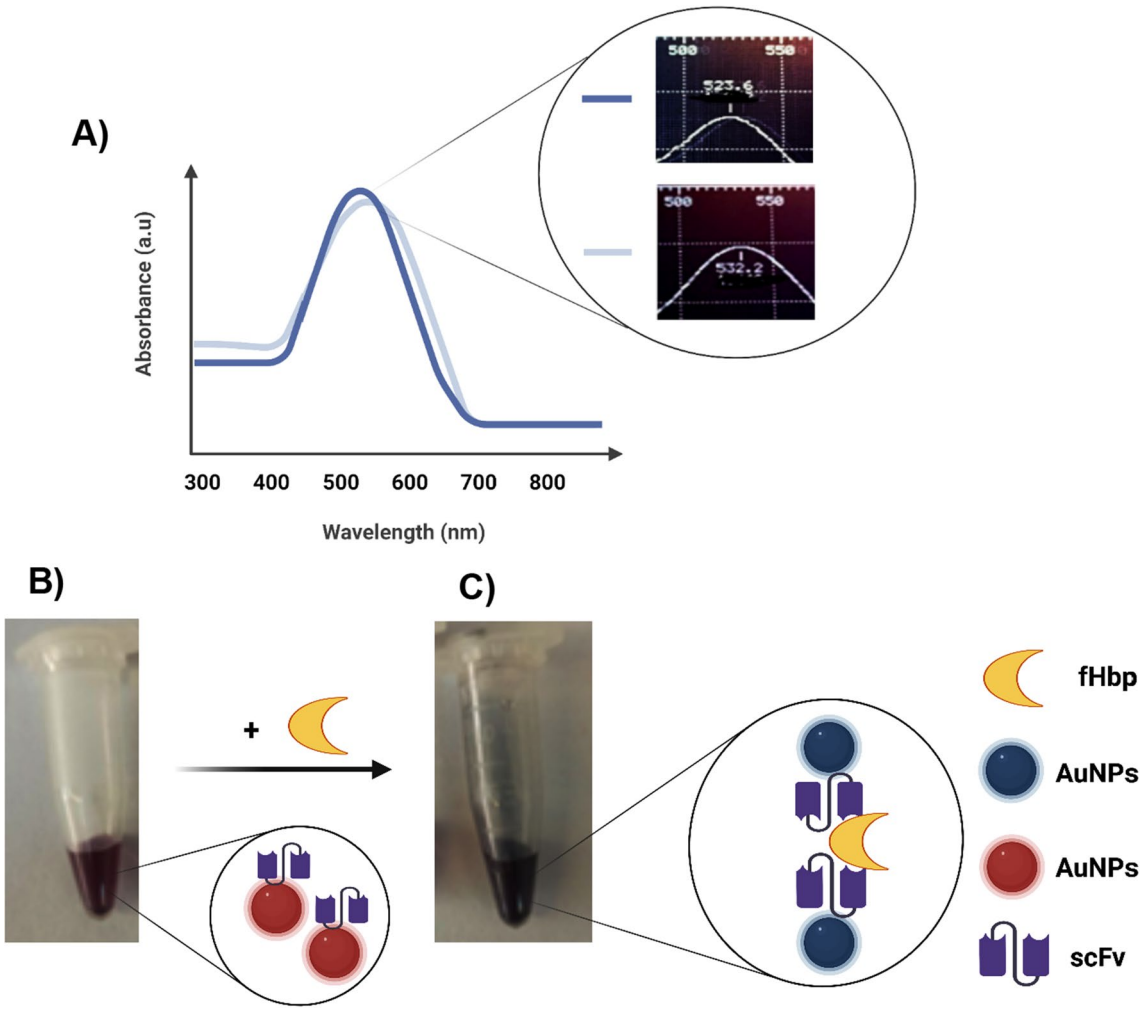

Fig. 6 **A** The surface plasmon resonance peak shift of the Au NPs from 523 (pure NPs: before conjugation to the scFv antibody) to 532 nm (after conjugation to the scFv antibody), and optical images along with schematic illustrations of the scFv-Au NP suspensions **B** before and **C** after adding *Neisseria meningitidis* pseudo lysate. A red color change to brown color is observable

tests were performed for two different concentrations of bacterial lysates of 0.5 and 1 µg/mL. However, for concentrations lower than 0.5 µg/mL no reliable color change could be detected. Hence, the limit of detection of the designed test stript was found ~ 0.5 µg/mL. To further confirm the selectivity of the test strip, the lysates of other bacteria, such as *Haemophilus influenza* (type b), *Listeria monocytogenes,* and *Mycobacterium tuberculosis* inducing meningitides, would be checked, in addition to the *E. coli* strains. The preliminary tests also indicated negative results for these bacteria.

3.5 Antibody-nanogold docking in silico

The energy minimization conducted in the Yasara server reported an energy change from—65,510 to − 116,900 kJ/mol (a score increase from − 1.74 to − 0.03). The *Z*-score (− 7.47) calculated with ProSA showed that our protein is in the range of all known *Z*-scores protein structures. Also, the results of the PROCHECK server for the Ramachandran plot confirmed that the scFv protein is in the favored regions. The *Z*-score plot consists of the Z-score of each experimental protein chain in PDB that has been specified via NMR spectroscopy, which is shown in dark blue, and X-ray crystallography, which is shown in light blue. Moreover, this plot represents the outputs with a *Z*-score ≤ 10. This protein *Z*-score is represented in the large black dot (Fig. 8). The docking report results confirm that the binding energy between the scFv and trisodium citrate on the surface of NPs is − 4.7 kcal. This shows that the gold nanoparticle atoms are in van der Waals interaction with Glu89, Gly123, and Gly122, in a hydrogen bond with Ser91, Ser88, Gly120, and Ser121, and also, there is a carbon -hydrogen bond with Arg40 (Fig. 9). The binding of antibodies to sodium citrate

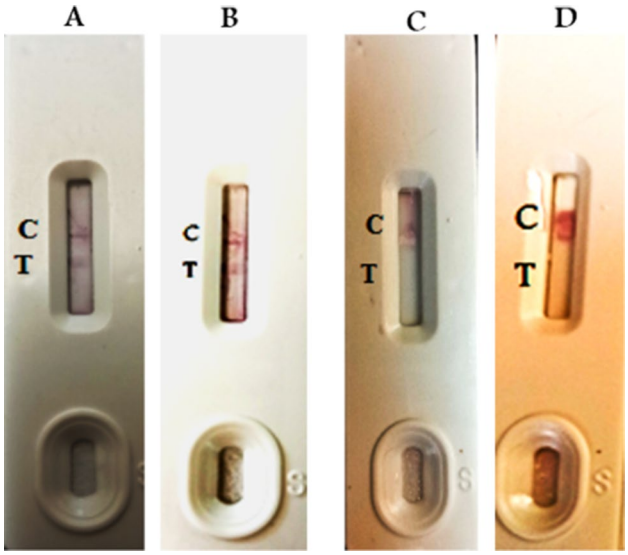

Fig. 7 Optical images of the strip tests. The positive results obtained after adding the pseudo lysate of the *Neisseria meningitidis* with various concentrations of **A** 0.5 and **B** 1 µg/mL, and the negative results obtained after adding *E.coli* with concentrations of **C** 0.5 and **D** 1 µg/mL

confirms the surface of the nanoparticles, clearly confirming the functionality and proper functioning of a conjugate of gold NPs and antibodies and, by its nature, the successful operation of the strip test.

4 Conclusions

The scFv recombinant antibody-Au NPs with average size of ~ 20 nm and red color were synthesized. The prepared NPs were loaded on nitrocellulose membrane pads for fabricating a selective lateral flow immunoassay test strip which is sensitive to the fHbp antigen of *Neisseria meningitidis*. The red color change to a brown color on both control and test lines was found after 3 min for 0.5 µg/mL of bacterial concentration (as the minimum detectable concentration). The docking method indicated that the Au NPs bounded to Glu89, Gly123, and Gly122 via van der Waals interaction, to Ser91, Ser88, Gly120 and Ser121 via hydrogen bonding, and to Arg40 via a C-H bonding. Meantime, the Z-score calculations confirmed the righness of the protein structures considered. These results can open up the commercial fabrication of a fast, simple, low-cost, portable and user-friendly test strip for *Neisseria meningitidis* bacterial detection.

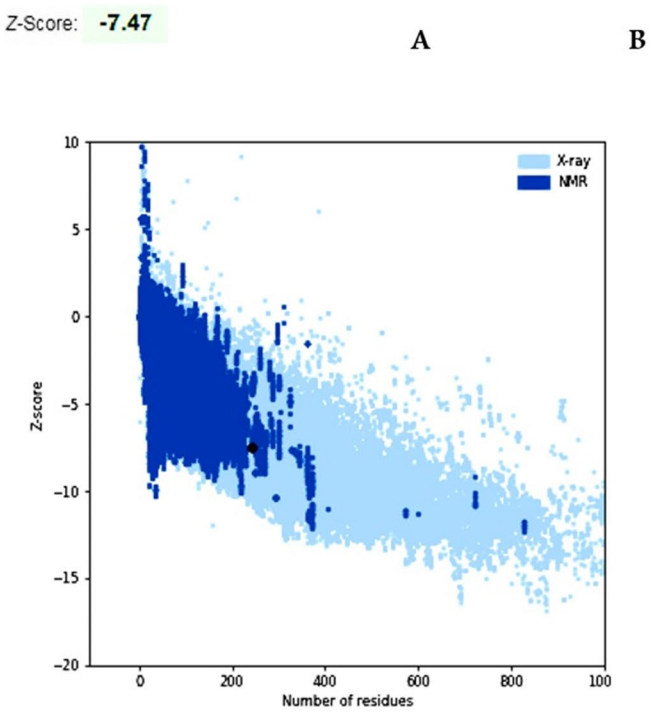

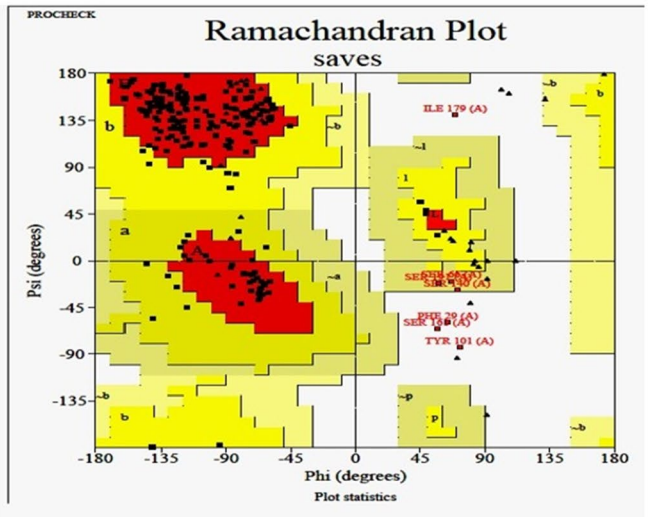

Residues in most favoured regions [A,B,L]	172	85.6%
Residues in additional allowed regions [a,b,l,p]	22	10.9%
Residues in generously allowed regions [~a,~b,~l,~p]	3	1.5%
Residues in disallowed regions	4	2.0%
Number of non-glycine and non-proline residues	201	100.0%
Number of end-residues (excl. Gly and Pro)	2	
Number of glycine residues (shown as triangles)	31	
Number of proline residues	9	
Total number of residues	243	

Fig. 8 **A** Validation of the scFv protein with the use of a ProSA-server. The scFv *z*-score (black dot) is located within the range of scores (− 7.47) which is usually observed for the native proteins with a similar size, and **B** validation the recombinant scFv with the Ramachandran plot by PROCHECK server. For the scFv, 172 residues (85.6%) are situated at the desired area, 25 residues (12.4%) in the permissible area, and four residues (2%) in the outlier area. In fact, 98% of the protein residues are in reasonable areas

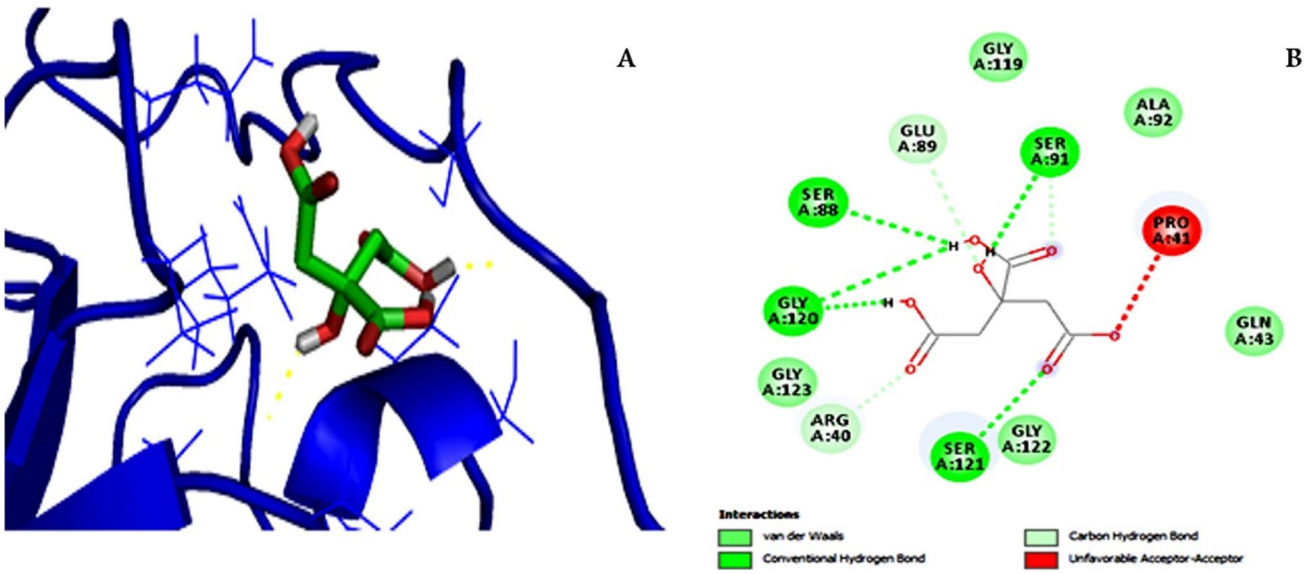

Fig. 9 **A** An schematic representation for the molecular structure of the scFv-Au NPs and **B** the amino acids including Ser91, Glu89, Ser88, Gly120, Gly123, Arg40, Ser121, and Gly122 involved in the bonding

Acknowledgements The authors of the article thank Shahid Beheshti University, Shahid Beheshti Medical Sciences, and Shahid Beheshti Cell and Molecular Biology Research Center for providing the necessary facilities. Also, biorender for design some of pictures (Created with BioRender.com).

Funding This study was supported by Iran National Science Foundation [Grant number: 91002087].

Declarations

Conflict of interest The authors confirm that there is no conflict of interest.

Ethical approval All experimental protocols were approved by of Shahid Beheshti University of Medical Sciences Ethics Committee [Code of Ethics: IR. SBMU.RETECH.REC.1400.080].

References

1. A.R. Feagins, O. Ronveaux, M.-K. Taha, D.A. Caugant, V. Smith, K. Fernandez, L. Glennie, L.M. Fox, X. Wang, Next generation rapid diagnostic tests for meningitis diagnosis. J. Infect. **81**(5), 712–718 (2020)
2. A. Mosavi-Jarrahi, A. Esteghamati, F. Asgari, M. Heidarnia, Y. Mousavi-Jarrahi, M. Goya, Temporal analysis of the incidence of meningitis in the Tehran metropolitan area, 1999–2005. Popul. Health Metrics **7**(1), 1–7 (2009)
3. R. Ghotaslou, F. Yeganeh-Sefidan, B. Salahi-Eshlaqi, H. Ebrahimzadeh-Leylabadlo, Etiology of acute bacterial meningitis in Iran: a systematic review. Acta Med. Iran **53**(8), 454–61 (2015)
4. I. de Filippis, C.R. Nascimento, M.B. Clementino, A.B. Sereno, C. Rebelo, N.N. Souza, L.W. Riley, Rapid detection of *Neisseria meningitidis* in cerebrospinal fluid by one-step polymerase chain reaction of the nspA gene. Diagn. Microbial. Infect. Dis. **51**(2), 85–90 (2005)
5. Z. Nezafat, M.M. Karimkhani, M. Nasrollahzadeh, S. Javanshir, A. Jamshidi, Y. Orooji, H.W. Jang, M. Shokouhimehr, Facile synthesis of Cu NPs@ Fe3O4-lignosulfonate: Study of catalytic and antibacterial/antioxidant activities. Food Chem. Toxicol. **168**, 113310 (2022)
6. N. Rabiee, S. Ahmadi, O. Akhavan, R. Luque, Silver and gold nanoparticles for antimicrobial purposes against multi-drug resistance bacteria. Materials **15**, 1799 (2022)
7. M. Hegde, P. Pai, M.G. Shetty, K.S. Babitha, Gold nanoparticle based biosensors for rapid pathogen detection: a review. Environ. Nanotechnol. Monit. Manag. **18**, 100756 (2022)
8. P. Sangpour, O. Akhavan, A. Moshfegh, M. Roozbehi, Formation of gold nanoparticles in heat-treated reactive co-sputtered Au-SiO2 thin films. Appl. Surf. Sci. **254**(1), 286–290 (2007)
9. A. Assali, O. Akhavan, M. Adeli, S. Razzazan, R. Dinarvand, S. Zanganeh, M. Soleimani, M. Dinarvand, F. Atyabi, Multifunctional core-shell nanoplatforms (gold@ graphene oxide) with mediated NIR thermal therapy to promote miRNA delivery. Nanomed. Nanotechnol. Biol. Med. **14**(6), 1891–1903 (2018)
10. J. Khan, Y. Rasmi, K.K. Kırboğa, A. Ali, M. Rudrapal, R.R. Patekar, Development of gold nanoparticle-based biosensors for COVID-19 diagnosis. Beni-Suef Univ. J. Basic Appl. Sci. **11**(1), 1–11 (2022)
11. K. Omidfar, F. Khorsand, M.D. Azizi, New analytical applications of gold nanoparticles as label in antibody based sensors. Biosens. Bioelectron. **43**, 336–347 (2013)
12. S. Gandhi, I. Banga, P.K. Maurya, S.A. Eremin, A gold nanoparticle-single-chain fragment variable antibody as an immunoprobe for rapid detection of morphine by dipstick. RSC Adv. **8**(3), 1511–1518 (2018)
13. F. Yarian, B. Kazemi, M. Bandehpour, Identification and characterization of a novel single-chain variable fragment (scFv) antibody against *Neisseria meningitidis* factor H-binding protein (fHbp). J. Med. Microbiol. **67**(6), 820–827 (2018)

14. Y.-C. Yeh, B. Creran, V.M. Rotello, Gold nanoparticles: preparation, properties, and applications in bionanotechnology. Nanoscale **4**(6), 1871–1880 (2012)
15. N. Hanžić, T. Jurkin, A. Maksimović, M. Gotić, The synthesis of gold nanoparticles by a citrate-radiolytical method. Radiat. Phys. Chem. **106**, 77–82 (2015)
16. M. Sengani, A.M. Grumezescu, V.D. Rajeswari, Recent trends and methodologies in gold nanoparticle synthesis—A prospective review on drug delivery aspect. OpenNano. **2**, 37–46 (2017)
17. M.H. Hussain, N.F. Abu Bakar, A.N. Mustapa, K.-F. Low, N.H. Othman, F. Adam, Synthesis of various size gold nanoparticles by chemical reduction method with different solvent polarity. Nanoscale Res. Lett. **15**(1), 1–10 (2020)
18. J. Kimling, M. Maier, B. Okenve, V. Kotaidis, H. Ballot, A. Plech, Turkevich method for gold nanoparticle synthesis revisited. J. Phys. Chem. B **110**(32), 15700–15707 (2006)
19. S.H. Yoon, M.-J. Han, H. Jeong, C.H. Lee, X.-X. Xia, D.-H. Lee, J.H. Shim, S.Y. Lee, T.K. Oh, J.F. Kim, Comparative multi-omics systems analysis of *Escherichia coli* strains B and K-12. Genome Biol. **13**(5), 1–13 (2012)
20. S. Bereswill, A. Fischer, I. Dunay, A. Kühl, U. Göbel, O. Liesenfeld, M. Heimesaat, Pro-inflammatory potential of *Escherichia coli* strains K12 and Nissle 1917 in a murine model of acute ileitis. Eur. J. Microbiol. Immunol. **3**(2), 126–134 (2013)
21. O. Akhavan, E. Ghaderi, Copper oxide nanoflakes as highly sensitive and fast response self-sterilizing biosensors. J. Mater. Chem. **21**(34), 12935–12940 (2011)
22. M.K. Patel, P.R. Solanki, S. Seth, S. Gupta, S. Khare, A. Kumar, B. Malhotra, CtrA gene based electrochemical DNA sensor for detection of meningitis. Electrochem. Commun. **11**(5), 969–973 (2009)
23. S.K. Dash, M. Sharma, A. Kumar, S. Khare, A. Kumar, Carbon composite-based DNA sensor for detection of bacterial meningitis caused by *Neisseria meningitidis*. J. Solid State Electrochem. **18**(10), 2647–2659 (2014)
24. A.A. Al-Tubuly, *SDS-PAGE and Western Blotting. Diagnostic and Therapeutic Antibodies* (Springer, 2000), pp.391–405
25. D.S. Kim, Y.T. Kim, S.B. Hong, J. Kim, N.S. Heo, M.-K. Lee, S.J. Lee, B.I. Kim, I.S. Kim, Y.S. Huh, Development of lateral flow assay based on size-controlled gold nanoparticles for detection of hepatitis B surface antigen. Sensors. **16**(12), 2154 (2016)
26. K. Niu, X. Zheng, C. Huang, K. Xu, Y. Zhi, H. Shen, N. Jia, A colloidal gold nanoparticle-based immunochromatographic test strip for rapid and convenient detection of *Staphylococcus aureus*. J. Nanosci. Nanotechnol. **14**(7), 5151–5156 (2014)
27. D. Subara, I. Jaswir, Gold nanoparticles: synthesis and application for Halal authentication in meat and meat products. Int J Adv Sci Eng Inf Technol. **8**, 1633–1641 (2018)
28. J. Martínez, N. Chequer, J. González, T. Cordova, Alternative methodology for gold nanoparticles diameter characterization using PCA technique and UV-VIS spectrophotometry. Nanosci Nanotechnol. **2**(6), 184–189 (2012)
29. A.V. Petrakova, A.E. Urusov, A.V. Zherdev, B.B. Dzantiev, Gold nanoparticles of different shape for bicolor lateral flow test. Anal. Biochem. **568**, 7–13 (2019)
30. S. Chotithammakul, M.B. Cortie, D. Pissuwan, Comparison of single-and mixed-sized gold nanoparticles on lateral flow assay for albumin detection. Biosensors **11**(7), 209 (2021)
31. A. Babapour, O. Akhavan, R. Azimirad, A.Z. Moshfegh, Physical characteristics of heat-treated nano-silvers dispersed in sol–gel silica matrix. Nanotechnology **17**, 763 (2006)
32. M. Kamel, F. Salah, Z. Demerdash, S. Maher, S. Atta, A. Badr, A. Afifi, H. El Baz, Development of new lateral-flow immunochromatographic strip using colloidal gold and mesoporous silica nanoparticles for rapid diagnosis of active schistosomiasis. Asian Pac. J. Trop. Biomed. **9**(8), 315 (2019)

Authors and Affiliations

Maryam Rad[1] · Gholamhossein Ebrahimipour[1] · Mojgan Bandehpour[2,3,4] · Omid Akhavan[5] · Fatemeh Yarian[2,3,6]

✉ Mojgan Bandehpour
m.Bandehpour@sbmu.ac.ir; Bandehpour@gmail.com

✉ Omid Akhavan
oakhavan@sharif.edu

[1] Department of Microbiology and Microbial Biotechnology, Faculty of Life Sciences and Biotechnology, Shahid Beheshti University, Tehran, Iran

[2] Cellular and Molecular Biology Research Center, Shahid Beheshti University of Medical Sciences, Tehran, Iran

[3] School of Advanced Technologies in Medicine, Shahid Beheshti University of Medical Sciences, Tehran, Iran

[4] Department of Medical Biotechnology, School of Advanced Technologies in Medicine, Shahid Beheshti University of Medical Sciences, Tehran, Iran

[5] Department of Physics, Sharif University of Technology, P.O. Box, Tehran 11155-9161, Islamic Republic of Iran

[6] Department of Medical Biotechnology, School of Advanced Technologies in Medicine, Fasa University of Medical Sciences, Fasa, Iran